# Comparison between Visible Channel Sensor Gains on GMS Series Satellites

**Akihiro Uchiyama\* and Hiroshi Fujimura\*\***

**Abstract**

For the purpose of monitoring the visible data and comparing with each other among the GMS, the GMS-2 and the GMS-3, we investigated the light reflected by inland area in Australia. The results suggest that the gain of the GMS is rather lower than the other satellites. Futhermore, it is found that the gain of visible sensor for each satellite is almost constant and the remarkable long term trend of degradation is not found.

## 1. Introduction

The geostationary meteorological satellites have made possible to obtain homogeneous data globally in a few tens of minutes and are indispensable for the global observation system. As the geostationary satellites become an impotant equipment, the quantitative data are required in the many fields of the earth science. The data obtained by the GMS series satellites has been used as image data. The calibration for both visible and infrared sensors has not been sufficiently performed and the absolute calibration has not been performed especially for the visible sensors. A normalization procedure is only performed to adjust the differences among the four visible sensors and to eliminate stripes on the pictures.

The absolute calibration is a very difficult problem in the present stage. International Satellite Cloud Climatology Project (ISCCP)

\* Meteorological Satellite Center System Engineering Division.
\*\* Meteorological Satellite Center Satellite Operations Division (Present affiliation: Science and Technology Agency).

partially resolves this problem by the method of an inter-calibration between NOAA series satellites and the geostationary satellites. This method still does not resolve the problem of the absolute calibration and needs an absolute calibartion for one of the satellites at least.

Visible calibration procedure, which utilizes the sun and space as the reference targets, has not been performed operationally for the GMS, the GMS-3 and the GMS-3 up to the present. During the GMS post-launch test period, we investigated the quality of the visible data. As a result, we found that the solar observation from the GMS was not stable and we cannot observe the sun during the eclipse periods. Furthermore, we found that "stripes" occured due to the differences of sensitivity between detectors. At that time, we were interested in a relative distribution of reflected radiances and not a derivation of physical and meteorological parameters from the visible data. Therefore, it was decided to eliminate the stripes from the visble pictures rather than to perform a

radiometric calibration. Until now, we have not yet obtained any information on the pre-launch test except for the conversion table of "albedo" to output voltage. It is described in the document that each visible channel was calibrated for each of the 9 "VISSR calibrator albedo" levels. The "VISSR calibrator" is a special equipment for the pre-launch test. We have not been provided with any information about this instrument.

In this study, we select target areas on the earth and investigate the time variation of light reflected by those areas for the purpose of monitoring the visible data and comparing with each other among the GMS, the GMS-2 and the GMS-3. The results suggest that the gain of the GMS fell down after the launch and the long term degradation for visible sensor is small. Our method enables us to investigate the differences of gain among the satellites and the continuity of observation can be maintained using those results.

## 2. Observation by satellite

In this section, an observation by the satellite in the range of visible wavelength and the relationship between the pre-launch test results and the observed data are briefly summarized.

(a) Pre-launch test

Only information that we have obtained on the pre-launch test is the tables of "albedo" ($A$) and sensor output voltage ($V$); these tables relate an energy into the instruments to a sensor output voltage. The quantity "albedo" is usually used for expressing the strength of the reflected light. This "albedo" is different from what we call albedo. Albedo is defined as a ratio of the reflected

flux to the incident flux;

$$A = \frac{\int_0^1 \int_0^{2\pi} I_\nu^+(\mu, \phi)\mu d\mu d\phi}{\mu_0 I_{\nu\,inc}} \qquad (2\text{-}1)$$

where $I_\nu^+(\mu, \phi)$ represents an upward intensity reflected into the direction of $\mu$ and $\phi$, $I_{\nu\,inc}$ represents intensity of sunlight incident on the top of the scattering layer and $\mu_0$ and $\nu$ are the cosine of solar zenith angle and a frequency, respectively. The albedo defined above is a monochromatic albedo and albedo for the all region of wavelength is defined as follows,

$$A = \frac{\int_0^\infty \int_0^1 \int_0^{2\pi} I_\nu^+(\mu, \phi)\mu d\mu d\phi d\nu}{\int_0^\infty \mu_0 I_{\nu\,inc} d\nu} \qquad (2\text{-}2)$$

Though no information on the pre-launch test has been provided in detail, it is inferred that when the pre-launch test and analysis was performed it was assumed that $I_\nu^+(\mu, \phi)$ is not dependent on $\mu$ and $\phi$. On the assumption of istropic reflection the pre-launch "albedo" is expressed as follows,

$$A = \frac{\pi \int_0^\infty I_\nu^+ d\nu}{\mu_0 \int_0^\infty I_{\nu\,inc} d\nu} \qquad (2\text{-}3)$$

Including the effect of instrument response function $\phi(\nu)$, eq. (2-3) can be rewritten as

$$\tilde{A} = \frac{\pi \int_0^\infty \phi(\nu) I_\nu^+ d\nu}{\mu_0 \int_0^\infty \phi(\nu) I_{\nu\,inc} d\nu} \qquad (2\text{-}4)$$

$$= \frac{\pi \tilde{I}^+}{\mu_{0g} \tilde{F}_s} \qquad (2\text{-}5)$$

where

$$\tilde{I}^+ = \int_0^\infty \phi(\nu) I_\nu^+ d\nu$$

$$\tilde{F}_s = \int_0^\infty \phi(\nu) I_{\nu\,inc} d\nu$$

$$\mu_{0g} = \mu_0$$

The sufix "$g$" represents the pre-launch test on the ground. The above expression for albedo shows that we need the knowledge on the frequency distribution of $I_\nu^+$, the frequency dependence of $\phi(\nu)$, and the information of $\mu_0$ in order to understand the results of pre-launch test. Hereafter, pre-launch "albedo" is distinguished from true albedo by adding double quotation marks.

  (b)  Relationship between sensor output and "albedo"

In the next step, we must relate the sensor output voltage ($V$) with the incident energy $\tilde{I}^+$. The instrument is desinged to hold the linear relationship between $V$ and $\tilde{I}^+$ ;

$$V = \alpha \cdot \tilde{I}^+ + V_0 \qquad (2\text{-}6)$$

where $V_0$ is an off-set voltage and $\alpha$ represent a gain.

Using equation (2-5) and (2-6), $A$ and $V$ are related by the following equation,

$$V = \alpha \cdot \frac{\mu_{0g} \tilde{F}_s}{\pi} \cdot \tilde{A} + V_0 \qquad (2\text{-}7)$$

$$= \alpha' \cdot \tilde{A} + V_0$$

In the period of pre-launch test, we measure the sensor output voltage ($V$) for the incident energy ($\tilde{I}^+$) which corresponds to "albedo" ($\tilde{A}$). Once $\alpha$ and $V_0$ are determined, we can get the relation between "albedo" and sensor output voltage. If there are two reference targets, $\alpha$ and $V_0$ can be determined. The on-board calibration usually utilize the sun and space as reference targets.

  (c)  Radiance observed by the satellite

The data transmitted from the satellite is the count value ($C$) which the sensor output voltage ($V$) is converted to. In the visible sensor for the GMS series satellite, the relationship between $C$ and $V$ are approximated by the following equation

$$C = \beta_0 + \beta_1 \cdot \sqrt{V} \qquad (2\text{-}8)$$

The count value is converted to sensor output voltage by this equation and then the sensor output voltage is converted to "albedo" by equation (2-7). However, the "albedo" obtained through the above sequence does not definitely mean a true albedo defined by eq. (2-3) and (2-4). The quantity observed by the satellite is a radiance reflected into the direction of the satellite. The radiance is obtained through sensor output voltage, equation (2-7) and the following equation,

$$\tilde{I}^+ = \frac{\mu_{0g} \tilde{F}_s}{\pi} \cdot \tilde{A} \qquad (2\text{-}9)$$

Using this averaged radiance, The bi-directional reflectance for the configulation of the sun and the satellite at the observation time is represented by the following equation,

$$\tilde{r} = \frac{\mu_{st} \tilde{I}^+}{\mu_0 \tilde{F}_s} \qquad (2\text{-}10)$$

where $\mu_{st}$ is satellite zenith angle and $\mu_0$ is the solar zenith angle at the time of observation.

Strictly speaking, the above description is not exact, because we do not refer to the spectrum ; there are differences among the spectrum of light source in the pre-launch test, that of reference target in the calibration procedure and that of reflected light. Furthermore, the gain of sensor is dependent on wavelength. The above equation relates the averaged radiance $\tilde{I}^+$ and "albedo" ($\tilde{A}$) on the condition that the detail of spectrum in the response function is not mentioned. We cannot infer the difference among the

spectra in the response function.

The relation between the sensor output voltage ($V$) and reflectivity ($\tilde{r}$) is rewritten,

$$V - V_0 = \alpha \cdot \frac{\mu_{0g}\tilde{F}_s}{\pi} \cdot \tilde{A}$$

$$= \alpha \cdot I^+$$

$$= \alpha \cdot \frac{\mu_0}{\mu_{st}} \cdot \tilde{F}_s \tilde{r}$$

$$= \alpha \cdot \frac{\mu_0}{\mu_{st}} \cdot \tilde{F}_s^* \cdot \left(\frac{r^*}{r}\right)^2 \cdot \tilde{r} \qquad (2\text{-}11)$$

where $r$ is the distance between the sun and earth, $r^*$ is the mean distance between them and $\tilde{F}_s^*$ is the value at the mean distance. $\tilde{r}$ is dependent on the position of the sun and the satellite. Therefore, the sensor output voltage is dependent on the zenith and azimuth angle of the satellite, those of the sun and the distance between the sun and the earth.

## 3. Data

The area which has the higher reflectance is a proper target. We selected the ground surface as the target area. The sea surface is not a proper target due to the lower reflectivity. The cloud has the high reflectance but the radiative property varies from cloud to cloud. Therefore, the cloud is not proper for the purpose of monitoring the gain of sensor over a long period.

Three target areas are selected in the inland of Australia. The dimension of a target area is 1° latitude×1° longitude and the centers of target areas are (20°S, 135°E), (25°S, 135°E) and (30°S, 135°E). The observational time is 03 Z and the data are extracted from the histogram data in the target area once a month. The histogram peak, which is composed of the data re-

flected from the ground, appears in the lower level part of histogram and we adopt the mode value of histogram as the data reflected from the ground. Examples of histogram are shown in Fig. 1 (a), (b) and (c). Fig. 1 (a) is an example of cloud free histogram. Fig. 1 (b) is an example of cloud contaminated histogram. In this case, the appearance of clouds in the target area causes the increase in the frequencies with both the higher and lower level. The increase in frequencies with the lower level sometimes occures due to the shawdow of cloud. Fig. 1 (c) is an example of cloudy histogram and data reflected by the ground cannot be extracted from this histogram.

Fig. 2 shows a variation of count value extracted by the above procedure. Each satellite has the different level but the annual variation is similar. The count value observed by the GMS, the GMS-2 and the GMS-3 is about twenty, twenty five and twenty three, respectively. Since the sensor gain was changed from the period of 29 June to 27 September in 1984 and data acquisition was not performed at 03 Z for that period, the data were not extracted. We analyzed not count value but sensor output voltage. The sensor output voltage is converted to digital count value and trasmitted to the ground station. The characteristics of electric circuit is being monitored by the method of inserting a 0 volt to 5 volt stair case response in the signal path. The electric circuit is stable and differences among the satellites are small. The count values are related to the voltages by eq. (2-8) and converted to sensor output voltage by using $\beta_0$ and $\beta_1$ in Table 1.

**Table 1** Parameters for visible calibration and normalization procedure. Note that the GMS visible channel #6 is not used for the failure of the detector.

| | | GMS | GMS-2 | | | GMS-3 |
|---|---|---|---|---|---|---|
| OPERATION PERIOD | | 87. 4. 1.00 Z<br>~81.12.21.06 Z<br><br>84. 1.21.09 Z<br>~84. 6.29.12 Z | 81.12.21.09 Z<br>~84. 1.21.00 Z<br><br>84. 6.29.18 Z<br>~84. 9.27.00 Z | | | 84. 9.27.06 Z<br>~UP TO DATE |
| SENSOR | | REDUNDANT | PRIMARY | | | REDUNDANT |
| REFERENCE CHANNEL | | CHANNEL #7 | CHANNEL #1 | | | CHANNEL #5 |
| $C=\beta_0+\beta_1*\sqrt{V}$ | $\beta_0$ | −0.23764 | −0.309 | | | −0.1321 |
| | $\beta_1$ | 27.728 | 28.375 | | | 28.37 |
| SUN COUNT VALUE | | 33 | 18.12.21<br>−48 | 82. 9. 7<br>−49 | 84. 6.29<br>−30 | 42 |
| SPACE COUNT VALUE | | 2 | 1 | 1 | 1 | 1 |
| SUN ALBEDO $(A_{SN})$ | | 30% | 55% | 42.5% | 48% | 45% |

## 4. Method

The variation of sensor output voltage are analyzed. The sensor output voltage can be converted to reflectivity through eq. (2-10). Eq. (2-11) can be utilized for removing the effect of the response function and the variation of the sun-earth distance. The analysis was performed on the following assumptions. Firstly, the seasonal variation of sensor output voltage observed by each satellite shows the same pattern. Secondly, since we cannot perform the absolute calibration, we choose the reference satellite and investigate the relative difference of sensor output voltage between the reference satellite and the others. Thirdly, the sensor sensitivity degrades exponentially with time. Finally, the off-set voltage $(V_0)$ is subtracted from the original sensor output voltage. The space view provides the zero percent albedo response and this sensor output voltage is regarded as an off-set voltage. Taking the above condition into consideration, the sensor output voltage can be written as follows,

$$V-V_0=A_n \exp(-b_n(t-t_n))$$
$$\times(C_0+C_1 \sin(\omega t)+C_2 \cos(\omega t)$$
$$+C_3 \sin(2\omega t)+C_4 \cos(2\omega t)$$
$$+C_5 \sin(3\omega t)+C_6 \cos(3\omega t))$$
$$(n=1, 2, 3) \quad (4-1)$$
$$\omega=\frac{2\pi}{12},$$

where coefficients with suffix "$n$" are dependent on the satellite, cofficients $C_i(i=0, \cdots, 6)$ are independent of the satellite and $t_n(n=1, 2, 3)$ is the operation start time of $n$-th satellite. The value of $A_n$ is taken as $A_n=1$ for the reference satellite. The term independent of satellite expresses the annual variation of reflected light with the period of a year, 6 months and 4 months. The GMS is selected as the reference satellite. The coefficients $A_n(n=2, 3)$, $b_n(n=1, 2, 3)$ and $C_n(i=0, \cdots, 6)$ are stepwisely determined by the following iterative procedure.
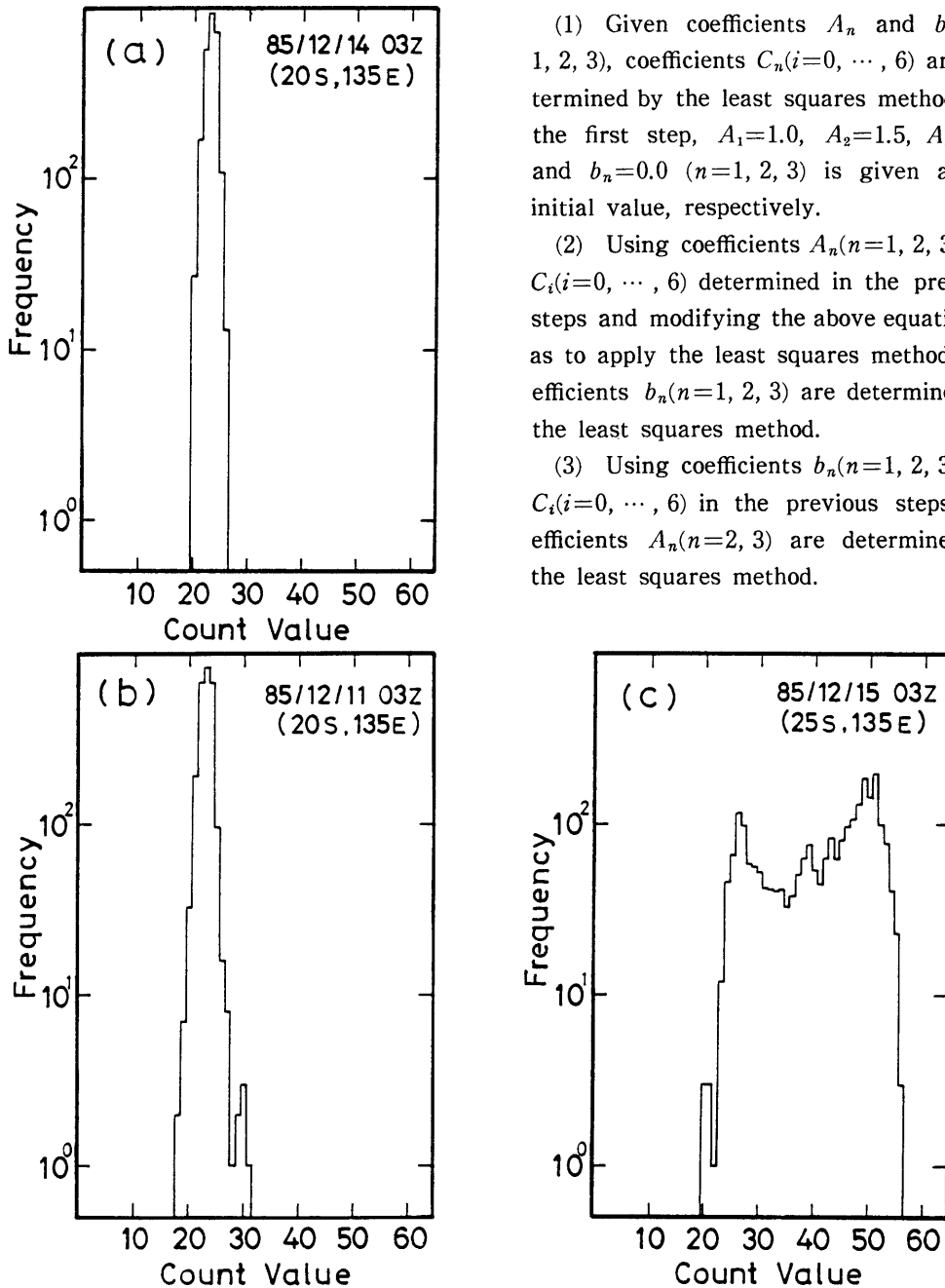
(1) Given coefficients $A_n$ and $b_n (n = 1, 2, 3)$, coefficients $C_n (i = 0, \cdots, 6)$ are determined by the least squares method. In the first step, $A_1 = 1.0$, $A_2 = 1.5$, $A_3 = 1.3$ and $b_n = 0.0$ $(n = 1, 2, 3)$ is given as an initial value, respectively.

(2) Using coefficients $A_n (n = 1, 2, 3)$ and $C_i (i = 0, \cdots, 6)$ determined in the previous steps and modifying the above equation so as to apply the least squares method, coefficients $b_n (n = 1, 2, 3)$ are determined by the least squares method.

(3) Using coefficients $b_n (n = 1, 2, 3)$ and $C_i (i = 0, \cdots, 6)$ in the previous steps, coefficients $A_n (n = 2, 3)$ are determined by the least squares method.

Fig. 1 Examples of visible data histogram in 1° (latitude) ×1° (longitude) area. Note that the ordinate is logarithmic scale.
(a) an example of cloud free histogram.
(b) an example of cloud contaminated histogram. The increase in frequency with both the lower and higher level occurrs. The lower part increase is caused by the shadow of cloud.
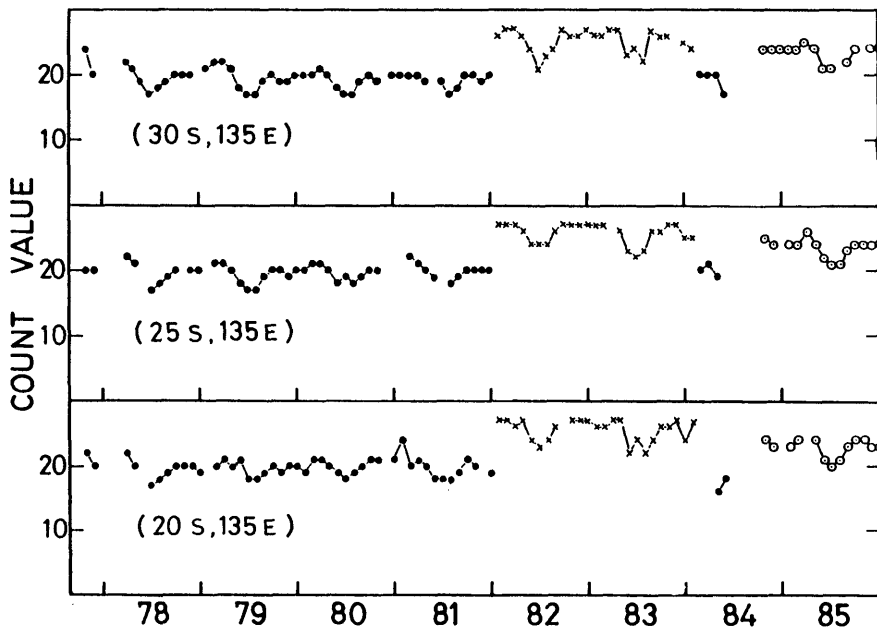(c) an example of cloudy histogram.

**Fig. 2** Time variation of observed count value. The target areas are selected in Australia inland area. Solid circle, GMS; cross, GMS-2; open circle, GMS-3.

**Table 2** Coefficients of eq. (4-1) stepwisely determined by the letst squares method. The inverse of $b_n (n = 1, 2, 3)$ indicates a time constant of visible sensor degradation. The long term degradation is very small.

| enter of Target | (20°S, 135°E) | (25°S, 135°E) | (30°S, 135°E) | Mean |
|---|---|---|---|---|
| $A_1$ | 1.0 | 1.0 | 1.0 | 1.0 |
| $A_2$ | 1.57 | 1.69 | 1.53 | 1.60 |
| $A_3$ | 1.17 | 1.35 | 1.25 | 1.26 |
| $b_1$ | 0.00271 | 0.00061 | 0.00239 | 0.00190 |
| $b_2$ | 0.00427 | 0.00303 | 0.00141 | 0.00290 |
| $b_3$ | 0.00007 | 0.00150 | 0.00004 | 0.00054 |
| $C_0$ | 0.559 E +00 | 0.519 E +00 | 0.542 E +00 | |
| $C_1$ | 0.584 E −01 | 0.610 E −01 | 0.681 E −01 | |
| $C_2$ | 0.198 E −01 | 0.115 E −01 | 0.895 E −02 | |
| $C_3$ | −0.384 E −01 | −0.412 E −01 | −0.421 E −01 | |
| $C_4$ | 0.243 E −01 | 00289 E −01 | 0.375 E −01 | |
| $C_5$ | −0.914 E −02 | 0.648 E −02 | −0.358 E −03 | |
| $C_6$ | −0.344 E −02 | −0.456 E −02 | −0.101 E −01 | |
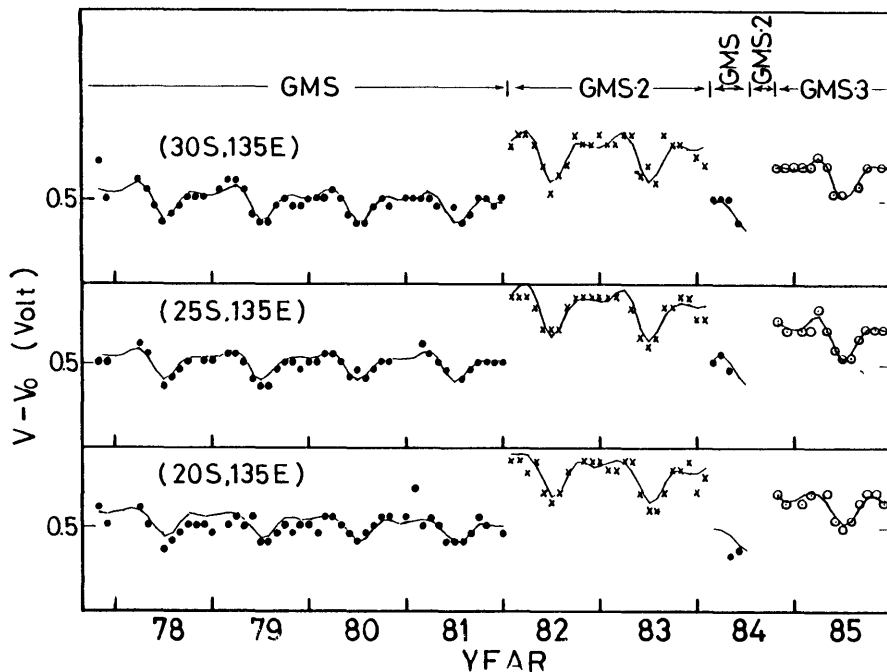
**Fig. 3** Time variation of sensor output voltage. Solid lines are fitting curves approximated by eq. (4-1) in text. Eq. (4-1) well expresses the variation of sensor output voltage.

**Table 3** The pre-launch results of visible sensor gain and off-set voltage. (a) scanner temperature = 20°C, (b) Scanner temparature = 10°C. The gain of the GMS-2 is about 10 percents higher than that of the GMS and the difference between GMS and the GMS-3 is less than 1 percent.

(a) Scanner Tem. = 20°C

| | | GMS | GMS-2 | GMS-3 |
|---|---|---|---|---|
| Scanner Temp. (°C) | | 19.52 | 19.9 | 19.8 |
| channel no. | | #7 | #1 | #5 |
| $V = \alpha \cdot A + V_0$ | $\alpha$ | 4.646 | 5.083 | 4.637 |
| | $V_0$ | 0.030 | 0.020 | 0.004 |
| Ratio of Gain | | — | 1.094 | 0.998 |

(b) Sconner Temp. = 10°C

| | | GMS | GMS-2 | GMS-3 |
|---|---|---|---|---|
| Scanner Temp. (°C) | | 9.55 | 8.0 | 10.3 |
| channel no. | | #7 | #1 | #5 |
| $V = \alpha \cdot A + V_0$ | $\alpha$ | 4.829 | 5.181 | 4.854 |
| | $V_0$ | 0.030 | 0.020 | 0.015 |
| Ratio of Gain | | — | 1.073 | 1.005 |

The above (1), (2) and (3) procedures are iterated and a convergence solution is seeked.

## 5. Results and discussion

The results of analysis are shown in Table 2. The solid lines in Fig. 3 are fitting curves. Eq. (4-1) well expresses the variation of sensor output voltage. Fig. 3 and the results of analysis obiously show that the gain of sensor on the GMS is rather lower than the gain of the other satellite. The comparison with coefficients $A_n(n= 1, 2, 3)$ shows that the gain of the GMS-2 and the GMS-3 is 1.6 times and 1.26 times as high as that of the GMS, respectively. The gains of visible sensor measured on the pre-launch test are shown in Table 3. The pre-launch relationship between "albedo" and sensor output voltage are shown in Fig. 4. The pre-launch test results show that the gain of visible sensor on the GMS-2 is 10 percents as high as that of the GMS and the difference between the GMS and the GMS-3 is less than 1 percent. These facts suggest that the gain of the sensor on the GMS had fallen after the pre-launch test. Fig. 5 shows a variation of "albedo" values which the count values are converted to using the coefficient in Table 1. Since it had not been ascertained that the gain of visible sensor on the GMS had fallen,
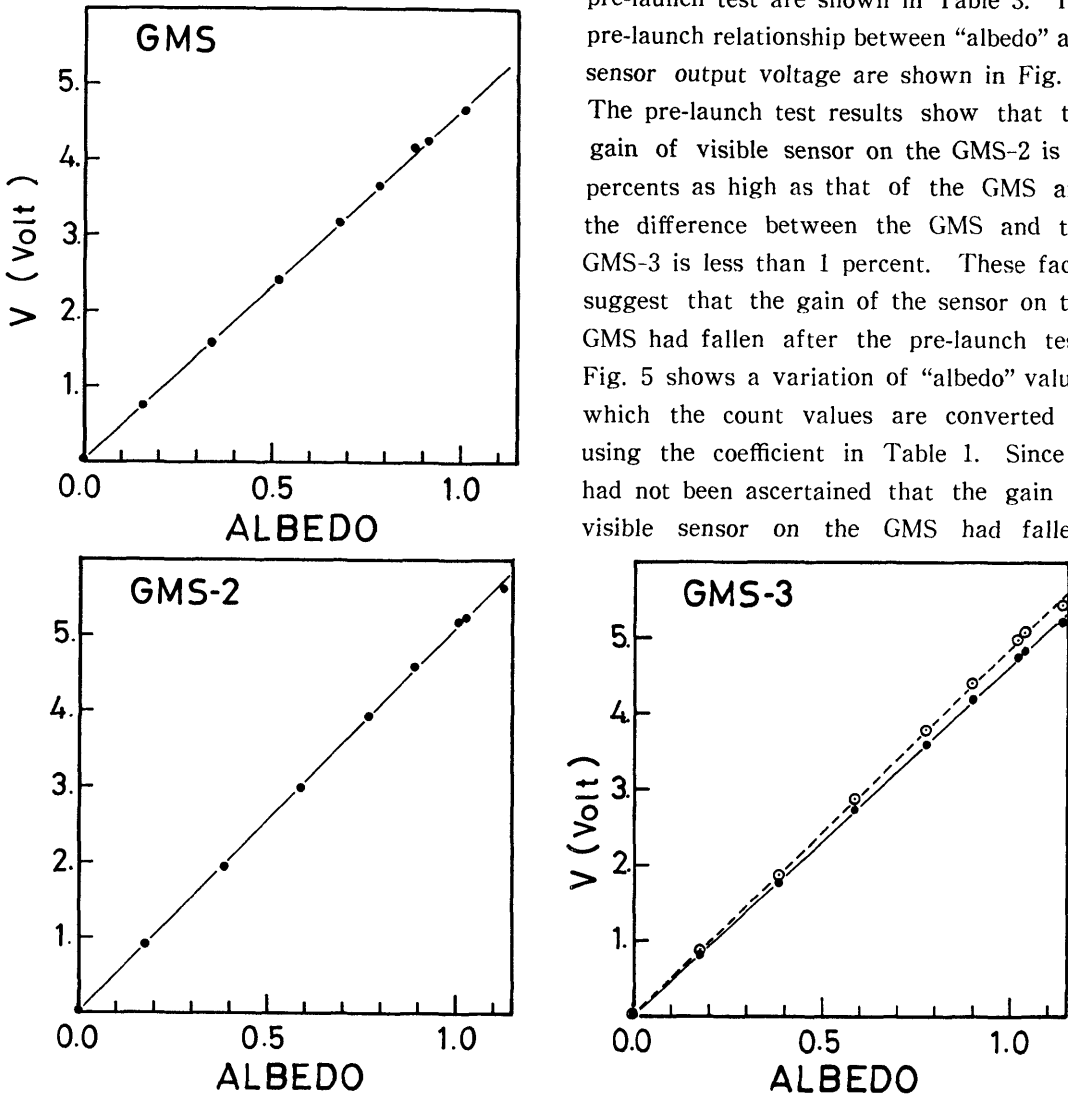


Fig. 4 Pre-launch results of relation between "albedo" and sensor output voltage. Solie circle, scanner temperature=20.0°C; open circle, scanner temperature=10.0°C.

"albedo" values in the look-up table had become lower than the actual values. After the launch of the GMS-2, it was found that the GMS-2 pictures were brighter than those of the GMS. The look-up table was reproduced in order to fit the GMS-2 brightness to that of the GMS on 7 September 1982 and then the lower "albedo" values were set in the look-up table for the GMS-2 as well as the GMS. Therfore, "albedo" values of the GMS-2 from January 1982 to August 1982 are larger than the values in the other operational period of the GMS-2.

The inverse of $b_n(n=1, 2, 3)$ can be considered as a time constant of the sensor degradation. The time constant of sensor degradation of the GMS is $526(=1/0.00190)$ months; i.e. 44 years. The time constant

of sensor degradation on the GMS-2 and the GMS-3 is 345 months and 1852 months, respectively. Though there are some dispersions in the results, these results show that the gain of visible sensor for each satellite is almost constant and the remarkable long term trend of degradation is not found. The sun count values, which are obtained through a prism for calibrating the visible data, gradually decrease with time; 1 to 2 counts/year for the GMS and 3 to 4 counts/ year for the GMS-2. The decrease of the sun count values is not caused by the degradation of the sensor gain.

The observed quantity shows an annual variation as seen from Fig. 2 and Fig. 3; the minimum values were observed in every June. This is partially caused from the
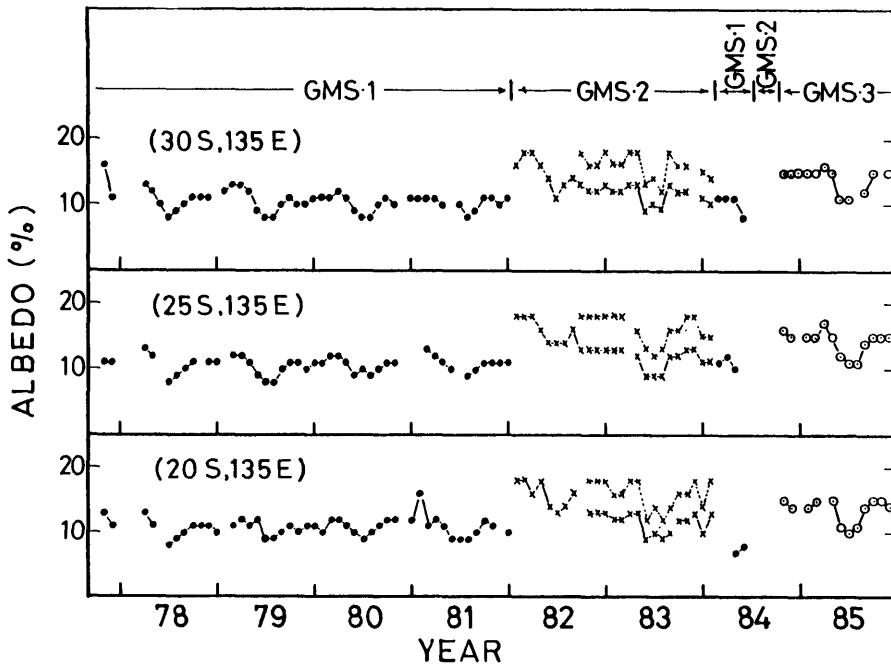


Fig. 5 Time variation of "albedo". Count value is converted to "albedo" using coefficients in Table 1. After 7 Sep. 1982, "albedo" value for the GMS-2 is fitted to the GMS one (see Table 1). The higher value after 7 Sep. 1982 is non-fitted "albedo"; i.e. "albedo" value is calculated using coefficient in the period from 21 Dec. 1981 to 7 Sep. 1982.

annual variation of the distance between the sun and the earth and partially from the variation of the solar zenith angle at the observed point. If the observed radiance is represented as a ratio of reflected radiance to the incident one, the look-up table to convert count values to "albedo" should be produced taking the variation of distance between the sun and the earth into consideration.

## 6. Conclusion

The method shown in this report enables us to investigate the differences of sensor gain among the satellites. The investigation of the reflected light from the target area on the earth surface suggests that the gain of the GMS fell down after the launch and the long term degradation for visible sensor is small. The annual variation of observed data is partially caused by the annual variation of the sun-earth distance. The look-up table to convert count value to "albedo" should be produced taking the annual variation of the sun-earth distance into consideration by means of eq. (2-11).

---

## GMS シリーズ衛星に塔載された可視チャネルの　センサー利得の比較

内　山　明　博*・藤　村　弘　志**

＊　　気象衛星センター　システム管理課
＊＊　　気象衛星センター　管制課（現所属，科学技術庁）

　GMS, GMS-2 と GMS-3 の可視チャネルによる観測値の監視のために，オーストラリアの内陸部に選んだ標的域からの反射光の時間変化を調べた。その結果，GMS の可視センサーの利得は GMS-2, GMS-3に比べてかなり低いことがわかった。更に，それぞれの衛星の可視センサーの利得の長期的な時間変化はほとんどないことがわかった。